

Isochoric Heat Capacity Measurements for 2,2-Dichloro-1,1,1-Trifluoroethane (R123) at Temperatures from 167 to 341 K and 1-Chloro-1,2,2,2-Tetrafluoroethane (R124) from 94 to 341 K at Pressures to 35 MPa

J. W. Magee¹

Received July 15, 2000

Molar heat capacities at a constant volume (C_v) of 2,2-dichloro-1,1,1-trifluoroethane (R123) and 1-chloro-1,2,2,2-tetrafluoroethane (R124) were measured with an adiabatic calorimeter. Temperatures ranged from 167 K for R123 and from 94 K for R124 to 341 K, and pressures were up to 33 MPa. Measurements were conducted on the liquid in equilibrium with its vapor and on compressed liquid samples. The samples were of a high purity, verified by chemical analysis of each fluid. For the samples, calorimetric results were obtained for two-phase ($C_v^{(2)}$), saturated liquid (C_σ or C'_x), and single-phase (C_v) molar heat capacities. The C_σ data were used to estimate vapor pressures for values less than 100 kPa by applying a thermodynamic relationship between the saturated liquid heat capacity and the temperature derivatives of the vapor pressure. Due to the tendency of both R123 and R124 to subcool, the triple-point temperature (T_{tr}) and the enthalpy of fusion ($\Delta_{fus}H$) could not be measured. The principal sources of uncertainty are the temperature rise measurement and the change-of-volume work adjustment. The expanded uncertainty (at the 2σ level) for C_v is estimated to be 0.7%, for $C_v^{(2)}$ it is 0.5%, and for C_σ it is 0.7%.

KEY WORDS: 1-chloro-1,2,2,2-tetrafluoroethane; 2,2-dichloro-1,1,1-trifluoroethane; heat capacity; R123; R124; vapor pressure.

1. INTRODUCTION

Accurate values of the heat capacity are valuable for establishing the behavior of the higher-order temperature derivatives of an equation of

¹ Physical and Chemical Properties Division, Chemical Science and Technology Laboratory, National Institute of Standards and Technology, Boulder, Colorado 80305-3328, U.S.A. E-mail: joe.magee@nist.gov.

state. In particular, the heat capacity at constant volume (C_v) is related to the equation of state $p(\rho, T)$ by

$$C_v - C_v^o = -T \int_0^\rho \left(\frac{\partial^2 p}{\partial T^2} \right)_\rho \frac{d\rho}{\rho^2} \quad (1)$$

where C_v^o is the ideal-gas heat capacity. At the present time, only one other report of heat capacity data for R123 and only one report (with 27 vapor-phase data points) for R124 were available. In this paper, new C_v measurements are reported for temperatures ranging from 94 to 341 K and pressures to 35 MPa.

2. MEASUREMENTS

2.1. Apparatus and Procedures

The adiabatic constant-volume calorimeter used for these measurements has been described in detail by Goodwin [1] and Magee [2]. For the heat-capacity measurement, a precisely determined electrical energy (Q) is applied and the resulting temperature rise ($\Delta T = T_2 - T_1$) is measured. The heat capacity is obtained from $C_v = (Q - Q_0 - W_{pV}) / (n \Delta T)$, where Q_0 is the energy required to heat the empty calorimeter, W_{pV} is the change-of-volume work that results from the slight dilation of the bomb, and n is the number of moles (obtained by weighing) enclosed in the bomb. Further details of this method are available in recently published work [2, 3].

2.2. Sample Purity

The purities of the components used to make the mixtures are an important aspect of this study. The manufacturer's stated purity of the R123 sample was 0.9999 mass fraction. The sample was poured from a metal screw-top container into a clean, dry Type-304 stainless steel vessel, which was filled to 25% of its volume with pretreated and dried molecular sieve pellets. A freeze-pump-thaw cycle was repeated five times to degas the sample. The liquid sample was dried over the sieve pellets for 2 weeks before its use in this study. The manufacturer's analysis of the R124 in our supply cylinder gave a purity of 0.999985 mass fraction. Samples of R124 were charged directly into our apparatus without further purification.

2.3. Assessment of Uncertainties

A detailed discussion of the uncertainties in the measured quantities is available in a recent publication [3]. We use a definition for the expanded

Table I. Expanded Uncertainties of Measurements with the Adiabatic Calorimeter

Temperature	0.03 K
Pressure	0.05 %
Density	0.15 %
Electrical energy	0.02 %
Change-of-volume work	0.2 %
Moles	0.002 %
Temperature rise	0.002 K
Heat capacity	0.7 %

uncertainty which is two times the standard uncertainty (a coverage factor $k=2$ and, thus, a 2-SD estimate). The expanded uncertainties of the original measurements and the resulting combined uncertainties are listed in Table I.

3. RESULTS

3.1. Heat Capacities

The heat capacity data of each run are presented in Tables II and III for two-phase states and in Tables IV and V for single-phase liquid states. The number of digits presented reflects the resolution of each measurement and is given to avoid round-off errors during a fit to a model. For the temperature, the average of the heating interval is given. In the single-phase liquid region, the pressures are calculated from pseudo-isochoric fits of the (p, T) -data of each isochore. For these fits, the temperature dependence of the equation of state of Jacobsen and Stewart [4] is used, with the density held constant. In the two-phase region, however, most of the measured vapor pressures are below the range of high-accuracy readings of the pressure gauge (3 to 70 MPa). For this reason, the pressures were calculated from vapor-pressure equations [5, 6] and are presented with footnotes *b* in Tables II and III. The density, given in Tables IV and V for single-phase liquid states, is calculated from the corrected number of moles and the bomb volume. In Tables II and III, values of the two-phase heat capacity at constant volume $C_v^{(2)}$ are presented as well as the saturated liquid heat capacity C_σ [also known as $C'_x = T(dS'/dT)$]. Values of C_σ are obtained by adjusting $C_v^{(2)}$ data with the equation given by Rowlinson [7],

$$C_\sigma = C_v^{(2)} - \frac{T}{\rho^2} \frac{d\rho_\sigma}{dT} \frac{dp_\sigma}{dT} + T \left(\frac{1}{\rho_\sigma} - \frac{1}{\rho} \right) \frac{d^2 p_\sigma}{dT^2} \quad (2)$$

Table II. Two-Phase Heat Capacity $C_v^{(2)}$ and Heat Capacity of Saturated Liquid C_σ of R123

T_{avg} (K)	$\rho_{\sigma, \text{avg}}^a$ (mol · L ⁻¹)	$p_{\sigma, \text{avg}}^{a, b}$ (MPa)	$C_v^{(2)}$ (J · mol ⁻¹ · K ⁻¹)	C_σ (J · mol ⁻¹ · K ⁻¹)
166.94	11.556	0.0000	137.83	137.82
171.10	11.490	0.0000	137.91	137.90
171.74	11.480	0.0000	138.08	138.07
174.88	11.431	0.0000	138.29	138.28
175.22	11.426	0.0000	138.32	138.31
178.01	11.383	0.0000	138.63	138.62
179.32	11.363	0.0000	138.46	138.45
181.60	11.328	0.0000	139.03	139.01
183.39	11.300	0.0000	138.84	138.82
185.65	11.265	0.0001	139.87	139.85
187.43	11.238	0.0001	139.19	139.17
189.68	11.204	0.0001	139.82	139.79
191.45	11.177	0.0001	139.84	139.81
193.68	11.143	0.0001	139.94	139.90
195.44	11.116	0.0002	140.06	140.02
197.66	11.083	0.0002	140.36	140.31
199.40	11.057	0.0003	140.49	140.43
203.34	10.997	0.0004	140.57	140.50
205.47	10.966	0.0005	141.42	141.34
207.25	10.939	0.0005	141.46	141.37
209.37	10.907	0.0006	141.67	141.57
211.14	10.881	0.0007	142.39	142.27
213.25	10.850	0.0009	142.56	142.43
215.01	10.823	0.0010	142.20	142.07
217.11	10.792	0.0012	142.66	142.51
218.86	10.766	0.0014	142.73	142.57
220.93	10.736	0.0016	143.25	143.07
222.68	10.710	0.0018	143.31	143.12
224.75	10.679	0.0021	143.89	143.68
226.48	10.654	0.0024	143.84	143.62
228.54	10.623	0.0028	145.16	144.92
230.26	10.598	0.0031	144.44	144.19
232.32	10.567	0.0036	144.97	144.70
234.02	10.542	0.0040	145.03	144.74
236.07	10.512	0.0045	144.90	144.59
237.75	10.487	0.0050	145.33	145.01
239.79	10.457	0.0057	145.45	145.11
241.47	10.432	0.0063	145.99	145.64
243.51	10.402	0.0072	146.23	145.86
245.17	10.377	0.0079	145.91	145.53
247.19	10.347	0.0089	147.01	146.62
248.84	10.323	0.0097	147.03	146.63
250.87	10.293	0.0109	147.63	147.21
252.51	10.268	0.0119	147.37	146.95
254.53	10.238	0.0133	147.56	147.13
256.14	10.214	0.0145	147.90	147.48

Table II. (Continued)

T_{avg} (K)	$\rho_{\sigma, \text{avg}}^a$ (mol · L ⁻¹)	$p_{\sigma, \text{avg}}^{a, b}$ (MPa)	$C_v^{(2)}$ (J · mol ⁻¹ · K ⁻¹)	C_σ (J · mol ⁻¹ · K ⁻¹)
258.16	10.184	0.0161	148.03	147.61
259.77	10.160	0.0174	148.83	148.41
265.39	10.075	0.0230	149.60	149.19
266.99	10.051	0.0249	150.01	149.62
268.97	10.021	0.0273	151.07	150.70
270.57	9.996	0.0294	150.28	149.95
272.55	9.966	0.0322	151.61	151.31
274.14	9.942	0.0346	150.90	150.64
276.11	9.912	0.0377	151.86	151.65
277.69	9.888	0.0404	152.35	152.19
279.65	9.857	0.0440	152.03	151.94
281.23	9.833	0.0470	152.98	152.95
283.18	9.802	0.0510	152.50	152.57
284.75	9.778	0.0544	153.09	153.23
286.69	9.747	0.0589	153.25	153.51
288.27	9.722	0.0627	153.80	154.15
290.19	9.692	0.0677	154.00	154.48
291.77	9.667	0.0720	154.68	155.28
293.69	9.636	0.0775	154.09	154.86
295.26	9.611	0.0822	155.20	156.11
297.16	9.581	0.0883	154.61	155.71
298.75	9.555	0.0936	155.27	156.54
300.64	9.524	0.1003	155.04	156.52
302.21	9.499	0.1061	156.55	158.24
304.09	9.468	0.1134	155.48	157.41
168.72	11.528	0.0000	137.80	137.80
172.57	11.467	0.0000	138.26	138.25
176.41	11.408	0.0000	138.61	138.61
180.22	11.349	0.0000	139.11	139.11
184.02	11.290	0.0001	139.40	139.40
187.79	11.233	0.0001	139.64	139.63
191.53	11.176	0.0001	139.74	139.74
195.26	11.119	0.0002	140.40	140.39
198.96	11.063	0.0003	141.09	141.08
202.64	11.008	0.0004	141.41	141.40
206.29	10.953	0.0005	141.68	141.68
209.93	10.899	0.0007	141.76	141.76
213.54	10.845	0.0009	142.03	142.03
217.14	10.792	0.0012	142.54	142.55
220.70	10.739	0.0016	143.23	143.25
224.26	10.686	0.0020	143.69	143.72
227.80	10.634	0.0026	144.10	144.15

^a Subscript avg denotes a condition evaluated at the average of the initial and final temperatures.

^b p_σ calculated from Ref. 5.

Table III. Two-Phase Heat Capacity $C_v^{(2)}$ and Heat Capacity of Saturated Liquid C_σ of R124

T_{avg} (K)	$\rho_{\sigma, \text{avg}}^a$ (mol · L ⁻¹)	$p_{\sigma, \text{avg}}^{a, b}$ (MPa)	$C_v^{(2)}$ (J · mol ⁻¹ · K ⁻¹)	C_σ (J · mol ⁻¹ · K ⁻¹)
94.28	14.034	0.0000	126.92	126.92
99.69	13.937	0.0000	127.18	127.18
103.27	13.872	0.0000	127.00	127.00
105.03	13.840	0.0000	127.26	127.26
108.55	13.777	0.0000	127.37	127.37
110.29	13.745	0.0000	127.12	127.12
113.75	13.683	0.0000	127.34	127.34
115.47	13.652	0.0000	127.32	127.32
118.88	13.590	0.0000	127.30	127.30
120.46	13.561	0.0000	127.17	127.17
120.57	13.559	0.0000	127.42	127.42
123.93	13.498	0.0000	127.21	127.21
125.49	13.469	0.0000	127.22	127.22
128.91	13.407	0.0000	127.21	127.21
130.46	13.378	0.0000	127.31	127.31
133.09	13.330	0.0000	127.67	127.67
133.84	13.316	0.0000	127.56	127.56
135.37	13.288	0.0000	127.56	127.56
137.96	13.241	0.0000	127.64	127.64
138.71	13.227	0.0000	127.79	127.79
140.21	13.199	0.0000	127.70	127.70
142.77	13.152	0.0000	127.87	127.87
143.52	13.138	0.0000	127.93	127.93
144.99	13.111	0.0000	127.60	127.60
147.53	13.064	0.0000	128.19	128.19
148.28	13.050	0.0000	128.27	128.26
149.73	13.023	0.0000	127.91	127.91
152.25	12.976	0.0000	128.13	128.12
152.99	12.962	0.0000	128.49	128.49
154.43	12.936	0.0000	128.20	128.20
156.92	12.889	0.0000	128.23	128.23
157.66	12.875	0.0000	128.97	128.97
159.07	12.849	0.0000	128.95	128.95
161.54	12.803	0.0001	128.88	128.87
162.28	12.789	0.0001	129.06	129.06
163.68	12.762	0.0001	129.21	129.20
166.12	12.716	0.0001	129.69	129.68
166.85	12.703	0.0001	129.62	129.61
168.23	12.677	0.0001	129.54	129.53
170.67	12.631	0.0002	130.26	130.25

Table III. (Continued)

T_{avg} (K)	$\rho_{\sigma, \text{avg}}^a$ (mol · L ⁻¹)	$p_{\sigma, \text{avg}}^{a, b}$ (MPa)	$C_v^{(2)}$ (J · mol ⁻¹ · K ⁻¹)	C_σ (J · mol ⁻¹ · K ⁻¹)
171.39	12.617	0.0002	130.14	130.13
172.75	12.591	0.0002	130.20	130.18
175.17	12.545	0.0003	130.67	130.65
175.83	12.532	0.0003	130.38	130.36
177.24	12.506	0.0004	130.43	130.41
179.62	12.460	0.0005	131.17	131.15
180.28	12.447	0.0005	130.91	130.88
181.68	12.421	0.0006	130.92	130.89
184.03	12.376	0.0007	131.52	131.49
184.70	12.363	0.0008	131.33	131.29
188.41	12.291	0.0011	132.04	131.99
189.08	12.278	0.0012	132.22	132.17
192.75	12.207	0.0016	132.80	132.73
193.43	12.194	0.0017	132.76	132.70
197.08	12.123	0.0023	133.54	133.46
197.74	12.110	0.0025	133.40	133.31
201.35	12.039	0.0033	133.67	133.57
202.01	12.026	0.0035	134.18	134.07
205.61	11.955	0.0045	134.45	134.32
206.27	11.942	0.0048	135.06	134.92
209.83	11.871	0.0062	135.37	135.22
210.48	11.858	0.0065	135.39	135.23
214.01	11.788	0.0082	136.06	135.87
214.67	11.775	0.0086	135.99	135.80
218.16	11.704	0.0108	137.10	136.88
218.81	11.691	0.0113	136.59	136.37
222.28	11.621	0.0140	137.18	136.92
222.94	11.607	0.0146	137.31	137.05
226.38	11.537	0.0179	137.70	137.41
227.03	11.524	0.0187	137.84	137.55
230.44	11.454	0.0227	138.43	138.10
231.10	11.440	0.0235	138.64	138.30
234.47	11.370	0.0283	139.48	139.10
235.15	11.356	0.0294	139.06	138.68
238.48	11.286	0.0351	139.95	139.54
239.16	11.272	0.0363	139.86	139.44
242.46	11.203	0.0430	140.51	140.05
243.15	11.188	0.0445	141.06	140.60
246.42	11.119	0.0521	141.74	141.25
247.11	11.104	0.0539	142.17	141.68

Table III. (Continued)

T_{avg} (K)	$\rho_{\sigma, \text{avg}}^a$ (mol · L ⁻¹)	$p_{\sigma, \text{avg}}^{a, b}$ (MPa)	$C_v^{(2)}$ (J · mol ⁻¹ · K ⁻¹)	C_σ (J · mol ⁻¹ · K ⁻¹)
250.36	11.034	0.0628	142.61	142.08
251.06	11.019	0.0649	143.19	142.65
254.26	10.950	0.0750	143.31	142.75
254.98	10.934	0.0774	143.56	143.00
258.15	10.864	0.0889	144.29	143.71
261.44	10.792	0.1023	145.30	144.69
262.02	10.779	0.1048	144.92	144.31
265.33	10.705	0.1200	145.48	144.86
265.86	10.693	0.1226	145.64	145.01
269.19	10.618	0.1399	146.54	145.91
269.69	10.606	0.1426	146.37	145.73
273.03	10.530	0.1621	147.97	147.33
273.50	10.519	0.1650	147.83	147.20
276.85	10.442	0.1868	148.80	148.17
277.28	10.432	0.1898	148.45	147.82
280.65	10.353	0.2143	149.91	149.31
281.04	10.343	0.2172	149.52	148.91
284.44	10.263	0.2445	150.80	150.23
284.79	10.254	0.2475	150.41	149.84
288.21	10.172	0.2779	151.30	150.77
288.51	10.164	0.2807	151.36	150.85
291.96	10.080	0.3143	152.81	152.35
292.22	10.074	0.3170	152.41	151.95
295.71	9.987	0.3543	153.44	153.06
295.92	9.982	0.3566	152.91	152.54
299.43	9.893	0.3977	154.09	153.82
299.60	9.889	0.3998	153.32	153.06
303.14	9.798	0.4449	155.36	155.22
303.26	9.795	0.4464	154.72	154.58
306.87	9.701	0.4960	155.74	155.75
306.93	9.699	0.4972	155.23	155.25
310.53	9.603	0.5511	156.85	157.04
310.56	9.602	0.5516	156.35	156.54
314.20	9.503	0.6105	158.03	158.42
314.20	9.503	0.6105	158.40	158.80
317.82	9.402	0.6737	159.89	160.53
317.85	9.401	0.6743	159.19	159.82

^a Subscript avg denotes a condition evaluated at the average of the initial and final temperatures.

^b p_σ calculated from Ref. 9.

where ρ_σ and p_σ are the density and the pressure of the saturated liquid and ρ is the bulk density of the sample residing in the bomb. The derivative quantities were calculated with the ancillary equations of Younglove and McLinden [5, 6].

The saturated liquid heat capacity C_σ , as a saturation quantity, depends on a single variable, temperature. If the data are internally consistent, then the values from different isochores must fall on a single curve. Though the C_σ values were evaluated from experiments with different amounts of sample in the calorimeter, the results should demonstrate consistency of all isochores. The saturated liquid heat capacities for all of the filling densities are depicted graphically in Figs. 1 and 2.

Values of the single-phase liquid heat capacity are shown in Figs. 3 and 4. The data are presented on isochores in a C_v - T diagram. Figures 3 and 4 show that both substances exhibit two behaviors in common. First, the slope of each C_v - T isochore is nearly independent of the density of the isochore. Second, the y -intercept obtained by passing a line through each C_v - T isochore increases with increasing density. Unlike dense-liquid states for other halogenated hydrocarbons in the same class (R125, R134a, R143a, R152a), the present heat capacities exhibit a strong dependence on fluid density.

Figure 11 in Ref. 5 shows comparisons of C_v and C_p for R123 with the equation of state of Younglove and McLinden. The absolute average deviation (AAD) for the C_v data from this work is 0.65%, with a bias of -0.73% . The AAD for the C_p data of Nakagawa et al. [8], not used in the fit, is 0.30%, with a bias of -1.37% . Figure 3 of de Vries et al. [9] shows comparisons of C_v for R124 with their fundamental equation of state for the reduced Helmholtz energy. The AAD for the C_v data from this work is 0.31%, with a bias of 0.11%. This is an excellent agreement. These comparisons show the exceptional quality of the published equation-of-state fits for both R123 and R124 data. Most of the calculated values of C_v are within 1% of the measurements.

3.2. Scanning for Triple Points

In previously reported studies of alternative refrigerant substances, experiments were carried out to measure the triple point temperature and the enthalpy of fusion. In the earlier work, the approximate temperature of fusion was measured by observation of a plateau on a temperature-time cooling curve. Then, the heating-scan measurements were started after the sample had been completely solidified and then cooled another 5 K below the triple point. However, for R123 and R124, no plateau was found during cooling scans. No success was found by reducing the rate of cooling to just

Table IV. Heat Capacity C_v for Liquid R123

T (K)	ρ_{avg}^a (mol · L ⁻¹)	P_{avg}^a (MPa)	C_v (J · mol ⁻¹ · K ⁻¹)
195.60	11.163	4.003	97.54
197.64	11.157	7.174	97.65
199.81	11.151	10.491	98.48
201.83	11.145	13.538	98.44
203.98	11.139	16.765	99.22
205.98	11.133	19.729	99.38
208.11	11.127	22.872	99.82
210.09	11.122	25.758	100.55
212.21	11.116	28.803	100.79
214.17	11.110	31.596	101.74
215.28	10.874	3.334	99.37
217.37	10.868	6.184	99.71
219.43	10.863	8.959	99.79
221.51	10.858	11.760	100.25
223.54	10.852	14.464	100.93
225.61	10.847	17.203	100.90
227.62	10.842	19.845	101.41
229.67	10.836	22.511	101.75
231.67	10.832	25.080	102.09
233.71	10.826	27.686	102.37
235.69	10.821	30.188	102.90
234.14	10.596	3.134	101.54
236.31	10.591	5.760	101.73
238.25	10.586	8.085	102.35
240.40	10.581	10.654	102.72
242.33	10.577	12.942	103.07
244.46	10.572	15.448	103.50
246.37	10.567	17.689	104.09
248.49	10.562	20.141	104.17
250.40	10.558	22.339	105.08
252.49	10.553	24.733	104.73
254.39	10.549	26.880	105.35
256.47	10.544	29.215	105.76
258.34	10.540	31.307	105.87
257.86	10.241	3.163	103.93
259.87	10.237	5.244	104.12
261.92	10.232	7.357	105.04
263.90	10.228	9.390	105.11
265.97	10.224	11.502	106.26
267.92	10.220	13.484	106.39

Table IV. (Continued)

T (K)	ρ_{avg}^a (mol · L ⁻¹)	P_{avg}^a (MPa)	C_v (J · mol ⁻¹ · K ⁻¹)
269.98	10.216	15.565	106.68
271.91	10.212	17.504	106.51
273.96	10.208	19.539	107.52
275.86	10.204	21.420	107.07
277.92	10.200	23.440	108.29
279.79	10.196	25.263	108.26
283.69	10.188	29.024	109.19
287.58	10.180	2.720	110.20
284.24	9.846	3.642	108.44
286.18	9.843	5.340	108.36
288.26	9.839	7.157	109.32
290.19	9.836	8.832	109.06
292.27	9.832	10.624	110.08
294.19	9.828	12.274	109.76
296.25	9.825	14.044	110.48
298.16	9.821	15.668	110.60
300.21	9.818	17.404	111.31
302.12	9.814	19.013	111.02
304.16	9.810	20.725	111.47
306.06	9.807	22.306	111.52
308.09	9.804	23.992	111.57
309.97	9.800	25.542	111.91
312.00	9.797	27.206	112.82
313.88	9.793	28.738	113.25
313.26	9.375	3.311	112.31
315.38	9.372	4.819	112.74
317.30	9.369	6.188	112.95
319.39	9.366	7.670	113.07
321.34	9.363	9.046	113.36
323.39	9.360	10.491	114.01
325.36	9.357	11.871	114.06
327.40	9.354	13.298	114.27
329.38	9.351	14.678	114.04
331.38	9.348	16.071	114.69
333.38	9.344	17.452	115.02
335.38	9.341	18.824	115.25
337.39	9.338	20.207	115.36
339.36	9.335	21.548	116.06
341.39	9.332	22.928	115.66

^a Subscript avg denotes a condition evaluated at the average of the initial and final temperatures.

Table V. Heat Capacity C_v for Liquid R124

T (K)	ρ_{avg}^a (mol · L ⁻¹)	P_{avg}^a (MPa)	C_v (J · mol ⁻¹ · K ⁻¹)
116.5965	13.668	6.740	88.19
119.0040	13.657	12.910	88.08
121.1077	13.647	18.215	88.54
123.4930	13.636	24.059	88.60
143.4199	13.164	6.584	87.27
145.7622	13.154	11.490	87.54
147.8117	13.146	15.747	87.73
150.1244	13.137	20.488	88.16
152.1503	13.129	24.578	88.33
154.4383	13.120	29.122	88.80
175.5699	12.571	6.831	88.95
177.6790	12.564	10.357	89.22
179.8410	12.557	13.937	89.77
181.9190	12.550	17.348	89.88
184.0637	12.543	20.838	90.21
186.1163	12.536	24.147	90.72
188.2472	12.529	27.543	90.97
209.9686	11.919	5.719	92.42
212.1008	11.913	8.519	92.58
214.1299	11.907	11.159	93.13
216.2286	11.901	13.869	93.50
218.2503	11.896	16.461	93.92
220.3302	11.890	19.111	94.19
222.3394	11.885	21.653	94.57
224.3903	11.879	24.229	95.01
226.3913	11.874	26.719	95.45
228.4211	11.868	29.221	96.05
230.4074	11.863	31.641	96.11
252.3937	11.042	2.982	97.83
254.3739	11.038	4.854	98.01
256.4831	11.034	6.842	97.80
258.4306	11.030	8.670	98.66
260.5242	11.025	10.627	98.70
262.4502	11.021	12.420	99.32
264.5703	11.017	14.384	99.45
266.4534	11.013	16.119	99.90
268.5792	11.009	18.068	99.63
270.4339	11.005	19.759	100.91
272.5609	11.000	21.688	100.62
274.4010	10.997	23.348	101.66
276.5152	10.992	25.244	101.56

Table V. (Continued)

T (K)	ρ_{avg}^a (mol · L ⁻¹)	p_{avg}^a (MPa)	C_v (J · mol ⁻¹ · K ⁻¹)
278.3513	10.988	26.882	102.28
280.4516	10.984	28.745	102.12
282.2811	10.980	30.359	102.72
283.2111	10.363	2.480	101.99
285.1519	10.360	3.896	102.35
287.2871	10.356	5.453	102.99
289.2120	10.353	6.853	103.41
291.3572	10.349	8.411	103.66
293.2472	10.346	9.779	104.24
295.4037	10.343	11.336	103.92
297.2748	10.339	12.682	104.80
299.4222	10.336	14.222	104.68
301.2813	10.333	15.550	106.07
303.4347	10.329	17.082	105.40
305.2807	10.326	18.390	106.04
307.4227	10.322	19.903	106.18
309.2498	10.319	21.188	106.15
311.4102	10.316	22.701	106.32
313.2258	10.313	23.968	106.78
315.3692	10.309	25.458	106.85
317.1876	10.306	26.718	107.57
319.3304	10.303	28.197	107.33
321.1330	10.300	29.436	107.69
323.2706	10.296	30.901	107.55
325.0516	10.293	32.117	109.25
327.1963	10.290	33.577	108.28
312.0871	9.651	2.316	106.46
314.2179	9.649	3.503	107.03
316.2212	9.646	4.616	107.48
318.3788	9.643	5.814	107.21
320.3540	9.640	6.909	107.53
322.5148	9.638	8.105	107.57
324.4609	9.635	9.181	107.51
326.6479	9.632	10.388	108.49
328.5598	9.629	11.441	108.45
330.7639	9.627	12.654	109.03
332.6566	9.624	13.692	109.60
334.8797	9.621	14.910	109.00
336.7574	9.619	15.936	109.81
338.9795	9.616	17.147	109.73
340.8486	9.613	18.163	110.42

^a Subscript avg denotes a condition evaluated at the average of the initial and final temperatures.

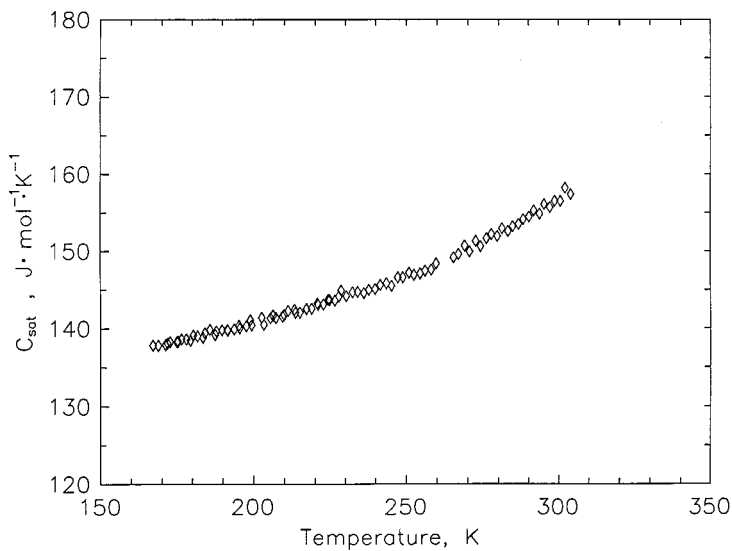


Fig. 1. Experimental saturated liquid heat capacity (C_{σ}) values for R123.

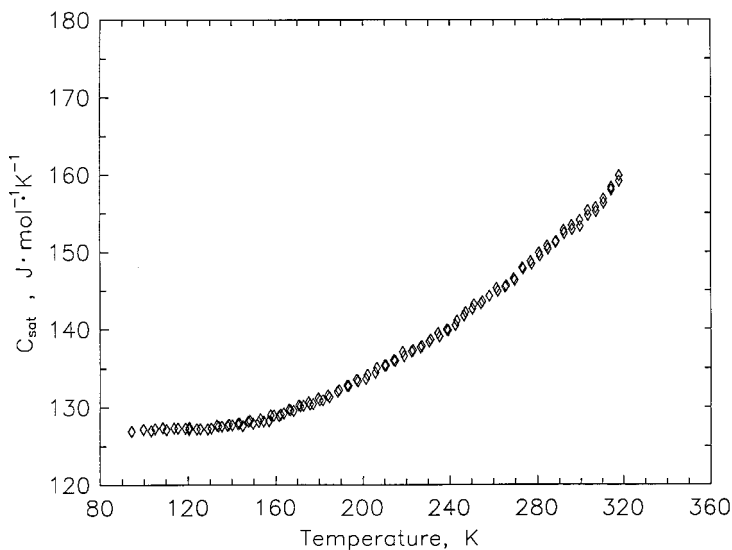


Fig. 2. Experimental saturated liquid heat capacity (C_{σ}) values for R124.

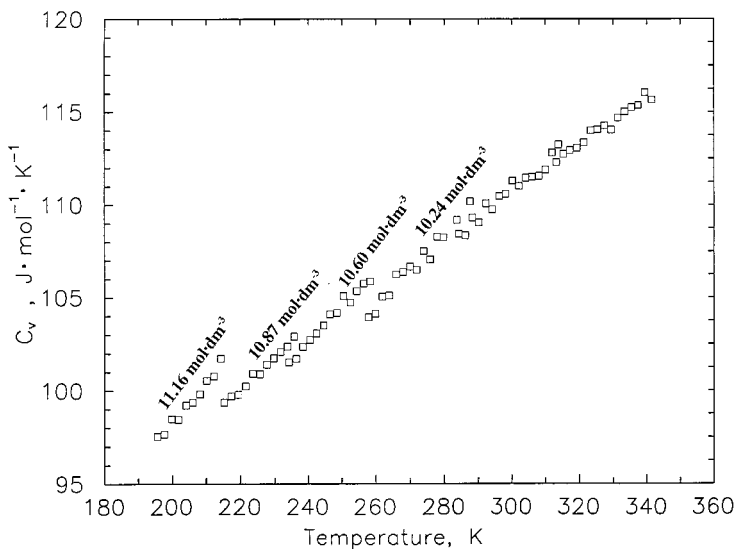


Fig. 3. Experimental liquid-phase heat capacity (C_v) data for R123.

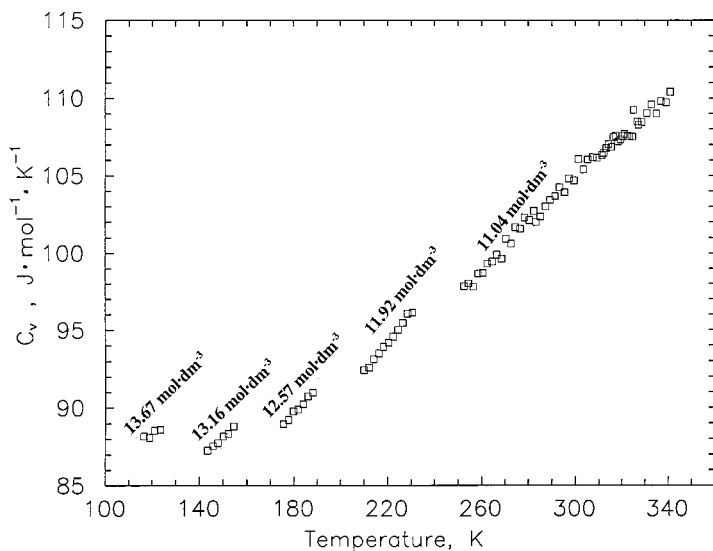


Fig. 4. Experimental liquid-phase heat capacity (C_v) data for R124.

$5 \times 10^{-4} \text{ K} \cdot \text{min}^{-1}$, which allowed cooling to proceed slowly over several days. At least three factors are responsible. The samples were of a very high purity, and thus there are too few seed crystals present in the liquid to promote solidification. The high molar mass of these samples means that molecules in the liquid phase near a triple point are in a very densely packed state. The structural asymmetry of these molecules leads to severe hindering of molecular rotation in a high-density state. With these factors in mind, the most likely explanation is that the change in molecular orientation from a random liquid to a solid matrix is not energetically favored; thus, the fluids form subcooled liquids in which the random orientation is locked in at low temperatures.

3.3. Derived Vapor Pressures

Vapor pressures measured between the triple point and the normal boiling point with traditional techniques are often inaccurate. In some cases, volatile impurities concentrate in the vapor phase [10]. This will influence the vapor pressure measurement, making it appear larger than the true value for the pure substance. In other instances, the pressure gauges are not accurate enough under these low-pressure conditions. This situation can be remedied to some extent, however, by extracting vapor-pressure values from saturated liquid heat capacity measurements. These C_σ values have a high internal consistency and can be accurate below the normal boiling point because the adjustments to the $C_v^{(2)}$ measurements are less than 2% of the resulting C_σ value. We extracted vapor pressures from the data in Tables II and III by applying a method recently applied by Weber [10] using the equation

$$C_\sigma \approx C' = C'' + \frac{RT}{V''} \left(\frac{dV''}{dT} \right) - T \left(\frac{dV''}{dT} \right) \left(\frac{dp}{dT} \right)_\sigma - V'' T \left(\frac{d^2p}{dT^2} \right)_\sigma \quad (3)$$

where C_σ denotes the saturated liquid heat capacity and the superscripts ' and '' denote saturated liquid and saturated vapor conditions, respectively.

These results are given in Table VI for R123 and in Table VII for R124. Because the method employed by Weber [10] requires a knowledge of the the density of the saturated vapor and its first temperature derivative, the expanded uncertainty (coverage factor $k = 2$) of the derived vapor pressures is estimated to be ± 0.05 kPa. Comparisons of the vapor pressures in Tables VI and VII are hindered by the absence of other published data in the same ranges of pressure. Nevertheless, some additional confidence in these results stems from two findings. First, Fig. 5 in Ref. 5 shows that the calculated vapor pressures for R123 smoothly join those

Table VI. Vapor Pressures Calculated from C_σ for R123

T (K)	p_σ (kPa)
170	0.0074
180	0.0278
190	0.0891
200	0.2488
210	0.6188
220	1.3946
230	2.8892
240	5.5670
250	10.075

directly measured with a sapphire ebulliometer by Goodwin et al. [11]. Also, Magee and Duarte-Garza [12] have shown that for a similar substance (R134a) for which reliable direct measurements are available, agreement with the calculated vapor pressures was within ± 0.02 kPa.

4. CONCLUSIONS

For 2,2-dichloro-1,1,1-trifluoroethane (R123) we have reported 79 C_v , 88 C_σ , and 9 p_σ values. For 1-chloro-1,2,2,2-tetrafluoroethane (R124), we have reported 82 C_v , 117 C_σ , and 13 p_σ values. Agreement with published liquid-phase heat capacity values at constant pressure was within 1% for R123. No published liquid-phase heat capacities were found for R124.

Table VII. Vapor Pressures Calculated from C_σ for R124

T (K)	p_σ (kPa)
140	0.002
150	0.011
160	0.046
170	0.163
180	0.488
190	1.271
200	2.955
210	6.245
220	12.167
230	22.123
240	37.918
250	61.759
260	96.248

ACKNOWLEDGMENTS

I am grateful to Mark McLinden and Ben Younglove for generous technical assistance with the calculations and many helpful discussions during this study. I have profited from many discussions with Gerald Straty and Marcia Huber. I am grateful to Mickey Haynes and Torsten Lüddecke for giving generously of their time to monitor long-term experiments and refill the liquid nitrogen Dewar during many nights and weekends while this work was carried out.

REFERENCES

1. R. D. Goodwin, *J. Res. Natl. Bur. Stand. (U.S.)* **65C**:231 (1961).
2. J. W. Magee, *J. Res. Natl. Inst. Stand. Technol.* **96**:725 (1991).
3. J. W. Magee, *Int. J. Refrig.* **15**:372 (1992).
4. R. T. Jacobsen and R. B. Stewart, *J. Phys. Chem. Ref. Data* **2**:757 (1973).
5. B. A. Younglove and M. O. McLinden, *J. Phys. Chem. Ref. Data* **23**:731 (1994).
6. B. A. Younglove and M. O. McLinden, personal communication (National Institute of Standards and Technology, Boulder, CO, 1992).
7. J. S. Rowlinson, *Liquids and Liquid Mixtures* (Butterworths, London, 1969), p. 37.
8. N. Nakagawa, H. Sato, and K. Watanabe, *J. Chem. Eng. Data* **36**:156 (1991).
9. B. de Vries, R. Tillner-Roth, and H. D. Baehr, *Proc. 19th Int. Congr. Refriger., Vol. IVa* (1995).
10. L. A. Weber, *Int. J. Refrig.* **17**:117 (1992).
11. A. R. H. Goodwin, D. R. Defibaugh, G. Morrison, and L. A. Weber, *Int. J. Thermophys.* **13**:999 (1992).
12. H. A. Duarte-Garza and J. W. Magee, *Int. J. Thermophys.* **18**:173 (1997).